

DIDLM: A SLAM Dataset for Difficult Scenarios Featuring Infrared, Depth Cameras, LIDAR, 4D Radar, and Others under Adverse Weather, Low Light Conditions, and Rough Roads

Weisheng Gong, Kaijie Su, Qingyong Li, Chen He, *Member, IEEE*, Tong Wu and Z. Jane Wang, *Fellow, IEEE*

Abstract—Adverse weather conditions, low-light environments, and bumpy road surfaces pose significant challenges to SLAM in robotic navigation and autonomous driving. Existing datasets in this field predominantly rely on single sensors or combinations of LiDAR, cameras, and IMUs. However, 4D millimeter-wave radar demonstrates robustness in adverse weather, infrared cameras excel in capturing details under low-light conditions, and depth images provide richer spatial information. Multi-sensor fusion methods also show potential for better adaptation to bumpy roads. Despite some SLAM studies incorporating these sensors and conditions, there remains a lack of comprehensive datasets addressing low-light environments and bumpy road conditions, or featuring a sufficiently diverse range of sensor data. In this study, we introduce a multi-sensor dataset covering challenging scenarios such as snowy weather, rainy weather, nighttime conditions, speed bumps, and rough terrains. The dataset includes rarely utilized sensors for extreme conditions, such as 4D millimeter-wave radar, infrared cameras, and depth cameras, alongside 3D LiDAR, RGB cameras, GPS, and IMU. It supports both autonomous driving and ground robot applications and provides reliable GPS/INS ground truth data, covering structured and semi-structured terrains. We evaluated various SLAM algorithms using this dataset, including RGB images, infrared images, depth images, LiDAR, and 4D millimeter-wave radar. The dataset spans a total of 18.5 km, 69 minutes, and approximately 660 GB, offering a valuable resource for advancing SLAM research under complex and extreme conditions. Our dataset is available at <https://gongweisheng.github.io/DIDLM.github.io/>

Index Terms—Multi-Sensor Dataset, challenging scenarios, Infrared Cameras, Depth Cameras, LiDAR, 4D Millimeter-Wave Radar

I. INTRODUCTION

SIMULTANEOUS Localization and Mapping (SLAM) is a pivotal technology in both autonomous driving and robotic self-mapping, orchestrating the construction of environmental maps alongside precise robot localization [1]. Its indispensable role in navigation, exploration, and collaborative tasks is self-evident. In uncharted geographic territories, SLAM ensures the accurate positioning of robots, a critical element for search and rescue operations as well as scientific expeditions. The fidelity of the constructed map data is essential for tasks such as environmental monitoring. Collaborative SLAM maximizes the synergistic potential of multi-robot systems. In environments devoid of GPS signals, SLAM emerges as a dependable guiding principle, assuring high-precision navigation. Its

This work was supported by the National Science Foundation of China 62271392, Shaanxi Innovation Team 2023CXTD04. (Corresponding author: Chen He.)

transformative impact extends to the realms of augmented and virtual reality. The profound influence of SLAM has propelled advancements in computer vision [2]. At its core, SLAM's essence lies in its remarkable capacity to enhance perception, navigation, and cooperation, thereby solidifying its stature as a foundational technology [3].

In the domain of outdoor SLAM, traditional laser SLAM often struggles with performance in adverse weather conditions such as rainy or snowy environments, while visual SLAM experiences significant accuracy degradation during snowy nights or in low-light conditions. In contrast, 4D millimeter-wave radar and infrared cameras have demonstrated robust capabilities in these challenging scenarios.

In addition, these sensors exhibit reduced robustness on bumpy terrains or smooth surfaces with speed bumps. There is a notable scarcity of dedicated datasets for 4D millimeter-wave and infrared camera data in conditions that include snowy, rainy weather, and roads with multiple speed bumps.

To enrich this field, we have introduced a variety of sensors and meticulously curated datasets from these extreme environments. This dataset provides support for professionals dedicated to researching multi-sensor fusion SLAM algorithms in these extreme conditions.

Our primary contributions are as follows:

- 1) Our dataset includes 4D millimeter-wave radar, infrared cameras, depth cameras, 3D LiDAR, RGB cameras, GPS, and IMU data. To our knowledge, there has been no previous work that includes all seven types of sensors and nine different types of information simultaneously.
- 2) The collected scenarios encompass complex conditions such as snowy weather, nighttime, rough terrains, and roads with speed bumps. To the best of our knowledge, this is one of the few datasets featuring seven types of sensor information under diverse weather, lighting, and road conditions for SLAM.
- 3) Our trajectories cover both structured and semi-structured terrains and include looped scenes to facilitate loop closure detection for SLAM systems. Reliable GPS/INS ground truth data is provided alongside raw data and processed TUM-format data, enabling users to select according to their preferences.
- 4) The dataset includes data collected from both ground robots and vehicles, catering to SLAM research for both robot navigation and autonomous driving. It spans large-scale and small-scale scenarios, with a total of 18.5 km, 69 minutes, and approximately 660 GB.



Fig. 1. The figure illustrates the actual ground robot and the vehicle equipped with sensors, with detailed labels indicating the function of each component. Additionally, the coordinates of each sensor are marked, with red representing the x-axis, green representing the y-axis, and blue representing the z-axis. It should be noted that within the scope of this manuscript, the 2D LiDAR and GNSS G-MOUSE depicted in the figure were not employed. Their application is reserved for separate endeavors.

- 5) We evaluate SLAM performance using all collected sensor types, including 4D millimeter-wave radar SLAM, LiDAR SLAM, infrared image SLAM, RGB image SLAM, Gaussian Splatting SLAM (based on depth images), and R3live SLAM. The challenges faced by each sensor under adverse environmental conditions are analyzed.
- 6) We conduct SLAM experiments across the sunny, rainy, and snowy weather conditions, the bright and dark conditions, the bumpy and not bumpy roads conditions, as well as the low and high (10-30 km/h) speed conditions. We compare SLAM trajectories with ground truth and analyzed them quantitatively using ATE and RPE metrics.
- 7) Additionally, we offer tools for converting LiDAR point clouds from CustomMsg to pointcloud2 and processing depth image boundaries, enabling users to utilize the dataset more efficiently.

II. RELATED WORK

Multi-sensor fusion has emerged as a prominent trend in the domain of SLAM, driven by the limitations of traditional single-camera or single LiDAR-based SLAM methods in addressing the intricacies of diverse environmental challenges, including those posed by varying weather conditions and terrains [4].

Sebastian Schramm et al introduced a novel SLAM algorithm in 2018 [11], which amalgamated depth and infrared cameras, facilitating joint SLAM operations even under low-light conditions. Building upon this, Chunran Zheng et al

TABLE I

THE TABLE ILLUSTRATES THE SCENARIOS AND TYPES OF DEVICES INCLUDED IN OUR LATEST DATASET. OUR DATASET ENCOMPASSES A VARIETY OF EXTREME CONDITIONS, INCLUDING SNOWY, RAINY, AND NIGHTTIME ENVIRONMENTS. IT ALSO COVERS ROADS THAT ARE SMOOTH YET EQUIPPED WITH SPEED BUMPS, AS WELL AS BUMPY TERRAINS, AND SITUATIONS INVOLVING GROUND MOVEMENTS OF BOTH ROBOTIC AND VEHICULAR ENTITIES.

Category	road conditions					Devices	
	day	night	rain	snow	bump	Robot	Car
KITTI	✓	✓					✓
RSRD	✓				✓		✓
M2DGR	✓	✓				✓	
Urbanloco [7]	✓	✓			✓		✓
RobotCar	✓	✓	✓	✓	✓		✓
4Seasons	✓	✓	✓	✓			✓
Brno Urban [9]	✓	✓	✓		✓		✓
NTU4DRadLM	✓	✓	✓			✓	✓
Goose	✓	✓	✓	✓	✓		✓
Boreas	✓	✓	✓	✓	✓		✓
ORD	✓	✓		✓			
DIDLM(ours)	✓	✓	✓	✓	✓	✓	✓

further advanced SLAM capabilities in 2022 [13] by integrating camera, IMU, and LiDAR data, thereby refining feature extraction techniques and enhancing SLAM precision. Concurrently, Jiarong Lin et al unveiled R3LIVE [14], a pioneering fusion methodology harnessing LiDAR for localization, IMU for positioning, and camera for capturing rich textural information, thus achieving commendable mapping outcomes. These efforts underscore the significance of multi-sensor fusion in elevating SLAM methodologies. Noteworthy examples of such advancements also include ORB SLAM3 [15], RGB-D SLAM [16], DM SLAM [17], and LIO-SAM [18].

The KITTI dataset [20], released in 2012 by Andreas Geiger et al, contains real image data collected from urban, rural, and highway scenes. Michael Burri et al published the EuRoC dataset in 2016 [21], which includes data from UAVs in indoor scenarios. In 2016, W. Maddern et al published "1 Year, 1000km: The Oxford RobotCar Dataset," which includes data from a 3D Lidar. 2016 [38] Schubert D et al released the TUM VI dataset in 2018 [22], providing indoor and outdoor datasets with handheld visual sensors and inertial measurement units. Matthew Pitropov et al introduced the 4Seasons dataset [8] in 2020 [23], covering challenging scenarios such as snowy conditions. Jie Yin et al presented the M2DGR dataset in 2021 [24], encompassing a wide range of indoor and outdoor scenes, diverse lighting conditions, and unique scenarios such as elevators. T. Sattler et al released the Seasons dataset in 2018 [25], which includes data from various weather and lighting conditions, although utilizing a relatively limited set of sensor types. In 2023, Tong Zhao et al [19] proposed a dataset targeted at road surface information and developed auxiliary algorithms beneficial for intelligent driving. In 2024 [12], Tong Zhao et al introduced the RSRD [12] dataset, which focuses on complex road conditions and incorporates data from LiDAR and visual sensors.

The work closest to ours is the NTU4DRadLM dataset, 2023, Jun Zhang et al, which includes a variety of sensors such as 4D millimeter-wave radar. However, due to geographical limitations, this dataset does not include snowy scenarios, which prevents the full demonstration of the advantages of

TABLE II

SENSOR TYPES IN THE DATASET. THE DATASET INCLUDES A SENSOR INVENTORY. COMMON SENSORS SUCH AS LIDAR, IMU, AND RGB CAMERAS ARE PRESENT, AND OUR DATASET ADDITIONALLY INCORPORATES 4D MILLIMETER-WAVE RADAR, INFRARED CAMERAS, AND DEPTH CAMERAS. STEREO: STEREO CAMERA.

Types	Lidar	4D radar	Stereo	Infrared	IMU	GPS
KITTI	✓				✓	
Tum VI			✓		✓	
M2DGR	✓			✓	✓	✓
Urbanloco	✓				✓	✓
RobotCar					✓	
4Seasons	✓				✓	✓
Brno Urban	✓			✓	✓	✓
Dual Radar	✓	✓				
View of Delft	✓	✓	✓		✓	✓
Goose	✓			✓	✓	✓
Boreas	✓				✓	✓
OORD	✓				✓	
NTU4DRadLM	✓	✓		✓	✓	✓
DIDLM(ours)	✓	✓	✓	✓	✓	✓

4D millimeter-wave radar and infrared cameras. Moreover, the NTU4DRadLM dataset lacks dedicated data collection for speed bumps and bumpy road sections. Additionally, the dataset is deficient in depth information from cameras. A comparison of various datasets is presented in Table 1.

For classic sensors such as cameras, LiDAR, and 3D millimeter-wave radar, we conducted thorough investigative analyses. Based on these analyses, we specifically designed data collection processes tailored to address complex scenarios that these sensors struggle to resolve.

- **CAMERA:** Cameras encounter several limitations including restricted field of view, sensitivity to lighting and texture, lack of depth information, motion blur, high computational costs, and geometric distortions. These factors may impede feature extraction and localization accuracy, particularly in complex environments.
- **LIDAR:** LiDAR encounters several limitations including high cost, susceptibility to weather conditions, motion distortion, occlusion issues, resolution constraints, and high power consumption. These factors may impede its accuracy in map construction and localization, particularly in complex environments.
- **3D-RADAR:** 3D millimeter-wave radar exhibits several limitations, including the inability to accurately measure object height, low resolution, and motion blur. Due to its inability to accurately measure object height, it cannot ascertain whether stationary objects ahead may impede vehicle passage. Additionally, its low resolution and susceptibility to motion blur may distort data accuracy when encountering high-speed movement or moving objects. Furthermore, its relatively low signal-to-noise ratio increases the likelihood of erroneous detections.

Using multiple sensors is effective in mitigating potential errors introduced by a single sensor. In the field of Simultaneous Localization and Mapping (SLAM), commonly used sensors include Inertial Measurement Units (IMUs), LiDAR, and cameras. However, when confronted with challenges in diverse environments, these sensors may fall short in supporting high-precision localization or mapping. The KITTI dataset, released in 2011 by Andreas Geiger et al, encompasses data from these

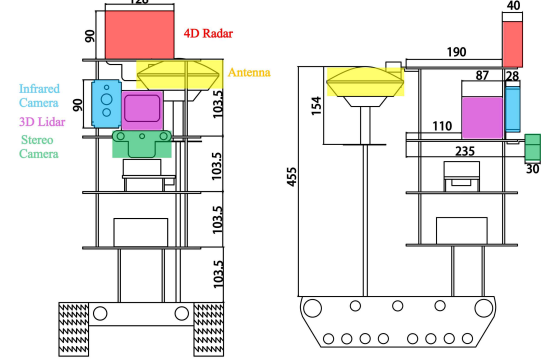


Fig. 2. Two-view diagram of the ground robot. Our ground robot uses a tracked movement system, which may allow it to better adapt to complex road conditions. unit:mm.

three sensor types. In 2021, Jie Yin et al published the M2DGR dataset, which incorporates IMUs, LiDAR, various cameras, and infrared cameras. Zhang X et al released an autonomous driving dataset in 2023 [26], which includes cameras, LiDAR, and two types of 4D millimeter-wave radar.

To diversify data types and enhance SLAM performance, as well as mitigate accuracy loss caused by extreme conditions for the aforementioned sensors, we have investigated and selected the following additional sensors:

- **4D millimeter-wave radar:** This sensor, an extension of the 3D millimeter-wave radar, includes height information. With strengths such as strong penetration, precise localization, and cost-effectiveness, it is considered a promising candidate to replace LiDAR. Our dataset incorporates a substantial amount of 4D millimeter-wave radar information, a rarity in current open-source datasets. We believe this addition will significantly aid researchers in related fields.
- **Infrared cameras:** These cameras can complement cameras and LiDAR in SLAM construction under conditions of excessive brightness or darkness. Particularly useful in scenes with significant variations in temperature, infrared cameras excel in tasks involving the identification of temperature-sensitive objects. Our dataset includes a considerable number of infrared images, contributing to improvements in SLAM accuracy and object recognition capabilities.
- **Stereo depth cameras:** Comprising two grayscale cameras and one RGB camera, these cameras provide both image and point cloud information simultaneously. We offer the intrinsic and extrinsic parameters of the three cameras in the stereo depth camera as a reference.

We have sorted out the sensor types contained in the currently available data set as shown in Table 2.

III. THE DIDLM DATASET

DIDLM stands for Difficult Scenarios Infrared Depth LiDAR Millimeter-wave, combining infrared cameras, depth cameras, 3D LiDAR, and 4D millimeter-wave radar to tackle complex environments with robust localization and mapping. We simultaneously build a ground robot and a vehicle containing the robot, which is fixed to the vehicle with a detachable

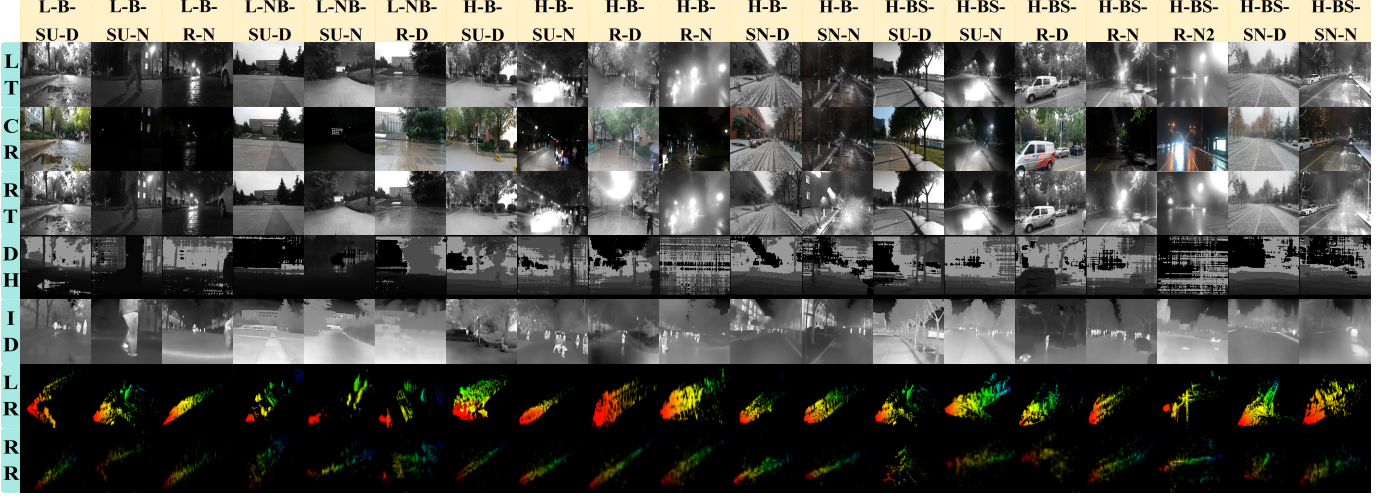


Fig. 3. The figure provides detailed information about the collected dataset. The dataset includes 19 different scenes and 9 types of sensors (the 7 types that can be visualized). LT: Left Camera, CO: RGB Camera, RT: Right Camera, DH: Depth Image, ID: Infrared Camera, LR: 3D Lidar, RR: 4D Radar. L: Low Speed, H: High Speed (10-30 km/h), B: Bumpy, NB: Non-Bumpy, BS: Bumps, SU: Sunny, R: Rainy, SN: Snowy, D: Day, N: Night.

device. The robot is divided into five layers, with the top three containing different sensors and the bottom two containing interfaces, wires, mobile power supplies and computers. The two views of the specific construction of the robot are shown in Figure 2; the types of data are shown in Figure 1 and 3.

A. Sensors setup

To achieve high-precision real-time localization, we utilized a dot matrix Livox [27] system to construct a three-dimensional laser point cloud. In addition, to acquire comprehensive data, we integrated a depth camera with an RGB camera to capture depth and image information from various perspectives. To address the challenges posed by adverse weather conditions and low-light environments, we augmented our setup with infrared cameras, ensuring accurate SLAM establishment under extreme conditions. Furthermore, we incorporated the latest 4D millimeter-wave radar sensor to enrich the construction of point cloud maps and to mitigate the impact of unfavorable weather on the development of localization maps.

Beyond ground-level data collection by the robot, all equipment was mounted on the roof of a vehicle to simulate high-speed data acquisition typical in autonomous driving scenarios. It should be noted that due to speed restrictions within the campus, our high-speed scenarios did not exceed 30 km/h. All our devices were synchronized to a unified clock source, and timestamps were obtained accordingly, with the maximum allowable time difference between sensor data being 0.05 seconds. The detailed information of the equipment is depicted in Figure 4. The sensors used in our study, along with their specifications, are presented in Table 3.

B. File format and topic name

We utilized the MCAP [28] system to record information from the Livox LiDAR, stereo camera, IMU. The GPS/INS information was saved in TXT files. All data was packaged into ROSBAG files. The ground truth format has been converted into the easily usable tum format, and the original format of

GPS/INS has also been included in the dataset for everyone's use. Detailed specifications for all topics can be found in Table 4. The data storage format is as follows:

```
data name.zip:
--color/compressed/Timestamps.png
--left/compressed/Timestamps.png
--right/compressed/Timestamps.png
--depth/Timestamps_depth.png
--infrared/Timestamps.png
--livox/lidar/Timestamps.pcd
--radar/Timestamps.pcd
--pointcloud/raw/Timestamps.pcd
--livox/imu/imu.txt
--GT.txt
--GTorig.txt
```

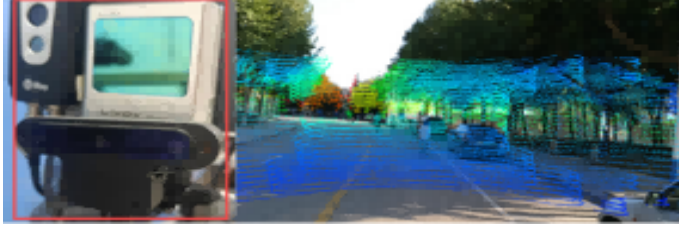
C. Sensor Calibration

Sensor calibration is crucial for ensuring the accurate utilization of data. In this section, we detail our calibration methods, processes, and results. Some of the picture is shown in Figure 5.

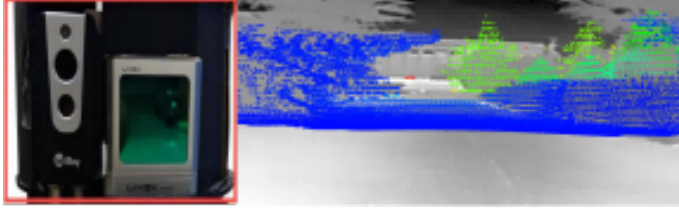
- 1) **Intrinsic Calibration of Cameras:** We employed Livox's official method [29] to estimate the intrinsic parameters. First, we printed a 5x6 chessboard calibration paper and affixed it flat on a wall. We captured approximately 20 images of the calibration board using the RGB camera and the left and right depth cameras. These images were then processed using calibration software to estimate the intrinsic parameters, which are recorded in the file `camera_intrinsics.yaml`.
- 2) **LiDAR to Camera Calibration:** We used Livox's official calibration method to initially calibrate the LiDAR with the RGB and depth cameras. Further manual adjustments were made using `SensorCalibration`. The three resulting extrinsic parameter files are stored in `lidar_to_rgb.yaml`, `lidar_to_left.yaml`, and `lidar_to_right.yaml`.

TABLE III
DETAILS OF THE SENSORS WE USED ARE PROVIDED. THE STEREO'S BASELINE IS 0.1136(M).

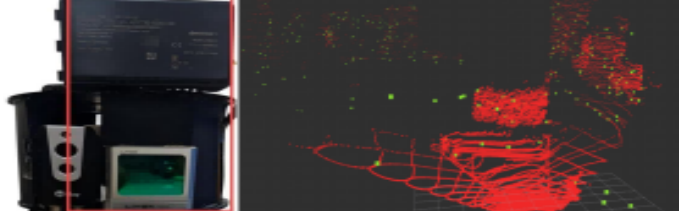
Category	Manufacturer	Type	Distance range	FOV (H × V × D)	Resolution	Special Spec.	Freq.
Lidar	Livox	Horizon	260m(± 2 cm)	81.7° \times 25.1° \times 0°	-	-	10HZ
imu	livox	BMI088	-	-	-	6-axis	200HZ
4D Radar	Continental	ARS548	0.2-301 m(± 0.15 m)	50° \times 20° \times 0° ± 0.1 ° ... ± 0.5 °	0.22m	-	20Hz
RGB	Luxonis	IMX378	-	69° \times 55° \times 81°	1920*1080(pixels)	-	30Hz
stereo	Luxonis	OV9282	0.7-12m(± 0.12 m)	72° \times 50° \times 82°	640*400(pixels)	-	30Hz
Infrared	InfiRay	AT20	-	56° \times 42° \times 0°	1024*768(pixels)	-20°C-550°C	25Hz
GPS	wheeltec	DETA100R	-	-	-	1m	200Hz
IMU	wheeltec	DETA100R	-	-	-	9-axis	400Hz



(a) LiDAR to Camera



(b) LiDAR to Infrared Camera



(c) Radar to LiDAR

Fig. 4. The figure includes the extrinsic calibration results from LiDAR to camera and infrared camera, as well as the extrinsic calibration results from LiDAR to radar. The red dense point cloud represents LiDAR point clouds, while the green sparse point cloud represents 4D millimeter-wave radar point clouds.

- 3) Intrinsic Calibration of the Infrared Camera: We utilized the principle that different colors have varying absorption and scattering capabilities for light and heat [30]. We reversed the colors of a black-and-white calibration board before printing it and captured approximately 20 images using the infrared camera for intrinsic calibration. The intrinsic parameters of the infrared camera are recorded in the file `infrared_intrinsics.yaml`.
- 4) LiDAR to Infrared Camera Calibration: We calibrated the extrinsic parameters using methods similar to those used for the LiDAR and cameras. The relevant data are stored in the file `lidar_to_infrared.yaml`.
- 5) IMU Intrinsic Calibration: We used `imu-utils` [31] for the intrinsic calibration of the IMU. Approximately 2 hours of IMU data were recorded, which was then used to calibrate the IMU's noise detection and random walk parameters. The data are saved in the file `imu.yaml`.
- 6) Camera to IMU Extrinsic Calibration: We employed `kalibr` [32] to calibrate the extrinsic parameters between

TABLE IV
OUR TOPICS, MESSAGE TYPES, AND SAMPLING FREQUENCIES ARE PROVIDED BELOW. EXCEPT FOR THE GPS/INS, ALL TOPICS HAVE BEEN RECORDED IN THE MCAP FORMAT.

Sensor	Topics	Message type	Rate
LiDAR	/livox/lidar	livox_ros_driver/CustomMsg	10Hz
	/livox imu	sensor_msgs/Imu	200Hz
Camera	/color/compressed	sensor_msgs/CompressedImage	30Hz
	/left/compressed	sensor_msgs/CompressedImage	30Hz
	/right/compressed	sensor_msgs/CompressedImage	30Hz
	/pointcloud/raw	sensor_msgs/PointCloud2	30Hz
	/depth	sensor_msgs/CompressedImage	30Hz
Radar	/ars548.detectionlist	-	20Hz
	/ars548.objectList	-	20Hz
Infrared	/infrared	sensor_msgs/Image	25Hz
GPS/INS	-	-	200Hz
GT(tum)	/timestamps	-	-
	/x, /y, /z	-	-
	/qx, /qy, /qz, /qw	-	-

the RGB camera, left and right depth cameras, infrared camera, and IMU. We collected about 2 minutes of multi-degree-of-freedom rotation and translation data and used `kalibr` for extrinsic calibration. The resulting file is `camera_to_imu.yaml`.

- 7) 4D Millimeter-Wave Radar to LiDAR Calibration: We manually calibrated the 4D millimeter-wave radar and LiDAR using `SensorCalibration`. The results are saved in the file `radar_to_lidar.yaml`.

D. Data Collection

To ensure the diversity of our dataset, we employed both low-speed and high-speed data collection methods. Our planned routes included uphill paths, semi-indoor environments, basements, plazas, bumpy roads, campus loops, and areas outside the campus. Most of these routes were covered under three weather conditions: sunny, rainy, and snowy, as well as two lighting conditions: daytime and nighttime. Our dataset includes continuous flat roads, continuous bumpy roads, and roads with multiple speed bumps. In summary, our dataset is purposefully designed with varying speeds, different road conditions, diverse weather, and lighting conditions, and features a rich set of sensors.

Firstly, we used ground robots to collect low-speed data at the same locations under different weather and lighting conditions. By maintaining consistent data collection locations while altering other conditions, we could analyze the impact of specific scenes on particular sensors, thereby facilitating SLAM algorithm improvement. We conducted low-speed data collection in open plazas with sparse walls and achieved loop closures on the route. Additionally, we gathered data in both above-ground and underground parking lots, characterized by numerous walls and vehicles. Subsequently, we collected data

TABLE V

THE TYPES OF DATA WE COLLECTED INCLUDE SPECIFIC DETAILS SUCH AS DISTANCE TRAVELED, RECORDING DURATION, TRAVELING SPEED, AND DATA SIZE. L:LOW SPEED, H:HIGH SPEED (10-30KM/H), B:BUMPY ROAD, NB:NON BUMPY ROAD, BS:BUMPS, SU:SUNNY, R:RAINY, SN:SNOWY, D:DAY, N:NIGHT.

Sequence	Distance (m)	Duration (s)	Speed (m/s)
L-B-SU-D	161	233	0.8
L-B-SU-N	217	260	0.9
L-B-R-N	257	270	1.0
L-NB-SU-D	377	585	0.7
L-NB-SU-N	331	352	0.9
L-NB-R-D	336	352	0.9
H-B-SU-D	158	29	5.5
H-B-R-D	190	31	6.2
H-B-SN-D	607	128	5.0
H-B-SU-N	194	40	5
H-B-R-N	193	38	5.0
H-B-SN-N	188	39	5.0
H-BS-SU-D	2386	314	2.8
H-BS-R-D	2409	288	6.0-10.0
H-BS-SN-D	2324	362	5.0-8.0
H-BS-SU-N	2319	349	5.0-8.0
H-BS-R-N	2352	320	6.0-9.0
H-BS-SN-N	2337	347	5.0-8.0
H-BS-R-N2	1476	130	12
total	18476	4115	-

on bumpy road sections, which posed challenges for loop closures due to their short distances; for more details, please see Figure 6.

Secondly, we mounted the robot on the roof of a vehicle, maintaining the same positions, to collect high-speed data under various weather and lighting conditions. We conducted high-speed data collection on roads with numerous speed bumps, providing significant insights for autonomous driving. Furthermore, we recorded sensor data while traversing bumpy road surfaces at high speeds.

We recorded approximately 1500 GB of image and point cloud data, which was subsequently converted to approximately 660 GB in .rosbag format and then uploaded to the data website. It should be noted that low light, strong turbulence, rain, snow, and other conditions can affect the imaging quality of cameras. We have compiled a list of the imaging quality for each sequence's RGB, left camera, right camera, and infrared camera, which is available on the data download website. Users can select camera topics with good imaging quality for algorithm testing based on the provided list. The overall data information is provided in Table 5. Some of the data recording processes have been documented, and videos may be uploaded to platforms for public viewing.

IV. EVALUATION

We performed SLAM tests using several state-of-the-art methods in their respective domains to analyze the challenges that still exist in current SLAM approaches. We ran LiDAR-based SLAM methods such as CT-ICP, Livox-SLAM, and visual SLAM methods like ORB-SLAM3, as well as infrared SLAM methods such as DSO-T and 4D millimeter-wave SLAM (4DRT-SLAM), in addition to depth image-based GS-SLAM. We also conducted tests on the tightly-coupled R3LIVE. The trajectory chart can be seen in Figure 13. We



Fig. 5. The left image is a picture of a section of the internal road of a school, with numerous cracks and potholes on the surface. Ground robots traversing this area would encounter significant jolts, and vehicles would experience substantial vibrations. Therefore, we designate this stretch as the bumpy road section. The right image is of a flat road, but with several speed bumps in the middle, which we name as the road with bumps section.

used metrics such as ATE (Absolute Trajectory Error) and RPE (Relative Pose Error) to evaluate the estimated trajectories, which can be seen at table 6.

A. Lidar SLAM

Livox-SLAM and CT-ICP [34] are among the most effective LiDAR-based SLAM algorithms in recent years and are highly compatible with Livox LiDAR. We first tested the impact of weather conditions (sunny, rainy, and snowy) on LiDAR-based SLAM performance using a dataset collected at speeds of 10–30 km/h with speed bumps. By comparing trajectory maps, we found that while the LiDAR SLAM algorithms performed well in sunny and rainy conditions, their accuracy significantly decreased under snowy conditions.

We quantitatively compared and analyzed the ATE and RPE for these three SLAM algorithms under different weather conditions. The experimental results indicate that snowy conditions significantly affect the positioning accuracy of LiDAR SLAM, while rainy and sunny conditions yielded similar results, with rainy conditions performing slightly better, likely due to reduced noise. However, the CT-ICP algorithm exhibited substantial errors under sunny conditions, likely due to anomalies in its loop closure and drift correction mechanisms. This hypothesis requires further validation.

Additionally, we visualized the LiDAR point clouds in snowy, sunny, and rainy conditions. The visualization reveals that in snowy conditions, both near and far LiDAR points were heavily affected by snowflake noise. This dense close-range noise significantly impacted the accuracy of the point

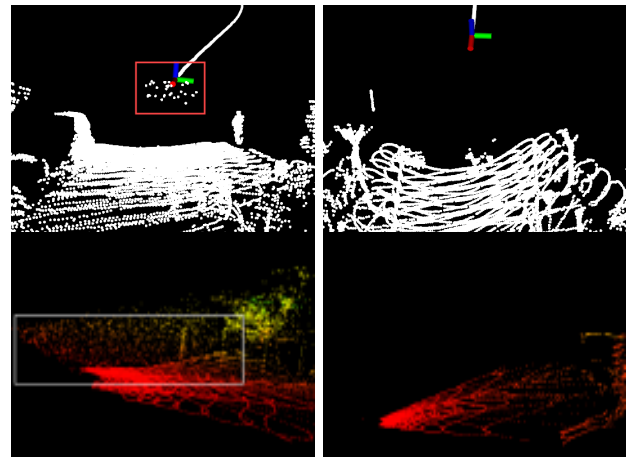


Fig. 6. The left image shows a LiDAR scan in a snowy scene with a large number of snowflakes obstructing the lens. The right images are comparisons with sunny weather, respectively.

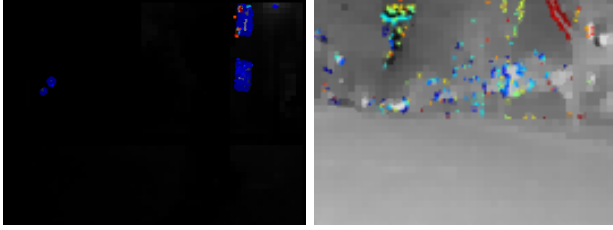


Fig. 7. The left and right figures show DSO-SLAM performance under low-speed-bumpy-sunny-night scenarios using RGB and infrared images, respectively. It is evident that infrared images generally provide better visibility and richer point clouds than RGB images at night.

cloud data. Future research on LiDAR SLAM may focus on mitigating the effects of snow on localization accuracy. For details, please refer to Figure 8.

Furthermore, the CT-ICP algorithm exhibited significant drift when traversing speed bumps on flat roads, which posed considerable challenges for subsequent mapping and loop closure tasks. While the other two algorithms did not show noticeable drift, they still experienced substantial errors in this environment. Effectively addressing sudden and intense jolts remains a critical issue for future LiDAR SLAM research.

B. Visual SLAM

ORB-SLAM3 is a visual SLAM algorithm that uses the ORB feature operator to extract keypoints, renowned for its fast response and precise feature extraction. In contrast, DSO-SLAM is a direct method that does not rely on feature points. To compare the accuracy of both methods in specific scenarios, we conducted tests using RGB images in environments with speeds ranging from 10 to 30 km/h, as well as low-speed conditions, across flat roads, multiple speed bumps, and continuously bumpy terrains. We also tested both methods in nighttime conditions, both with and without headlights. For safety reasons, the without headlights scenario was conducted at low speed.

The experiments showed that RGB images suffer from reduced robustness in scenarios involving continuous bumps or sharp turns. In environments with multiple speed bumps, excessive camera shake often led to feature tracking failures. Similarly, constructing visual SLAM trajectories in nighttime conditions without headlights proved to be highly challenging, while in headlights-on scenarios, feature points were often misdetected along the contours of the headlights.

Generally, feature-based mapping methods provide higher accuracy, while direct methods tend to outperform in terms of robustness. Ensuring sufficient feature recognition to complete SLAM in highly bumpy roads and low-temperature nighttime scenarios will likely be an important direction for future RGB image-based visual SLAM research.

C. Infrared SLAM

Infrared images provide rich thermal information, making them particularly useful in low-visibility scenarios such as nighttime conditions. However, due to the unique feature selection methods of infrared images, conventional SLAM algorithms like ORB-SLAM3 are not well-suited for infrared data. Direct methods, on the other hand, can typically find

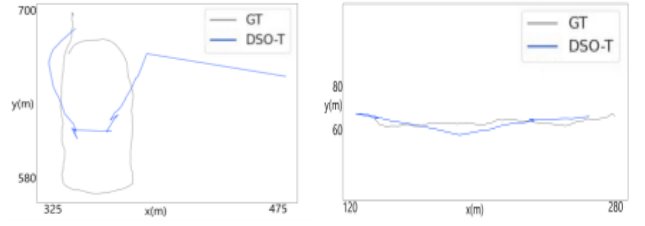


Fig. 8. The figure shows a comparison of the DSO-T(Thermal)-SLAM trajectory using infrared images at night with the ground truth (GT). It can be observed that, despite being able to map in nighttime conditions compared to RGB images that cannot perform mapping, the accuracy of the infrared image-based SLAM still needs improvement.

sufficient point cloud information for localization. However, due to the inherent limitations of direct methods, the SLAM accuracy is significantly compromised.

We tested DSO-SLAM on various nighttime scenarios with infrared images. Visually, the point cloud information in infrared images was much richer than that obtained from RGB images in similar nighttime conditions. Moreover, DSO-SLAM demonstrated robust performance in nighttime scenarios where RGB images failed to provide reliable localization and mapping. However, the localization accuracy was still quite low, indicating that further research is needed into feature point selection methods for infrared images.

Additionally, we found that the presence of objects with significant temperature differences, such as pedestrians, running vehicles, or plants, greatly improved the mapping performance of infrared SLAM. However, when these temperature-differentiated objects were absent, infrared SLAM often faced issues with a lack of available feature points or point clouds. Furthermore, continuous bumps or multiple speed bumps still significantly affected the performance of infrared SLAM.

In conclusion, while infrared SLAM shows promise, especially in low-visibility conditions, its feature point selection and robustness in dynamic environments remain critical areas for future research. The difference in point cloud selection between RGB and infrared images during nighttime DSO-SLAM is shown in Figure 9. The trajectory of DSO-SLAM using infrared images at night is illustrated in Figure 10.

D. 4D millimeter-wave radar SLAM

We utilized the latest 4D millimeter-wave radar, which offers advancements over traditional 3D radar by incorporating height information and, in some cases, Doppler velocity data. Leveraging its unique wavelength, the 4D millimeter-wave radar's point cloud effectively penetrates adverse weather conditions, including rain, snow, fog, and haze. To evaluate its performance, we specifically designed SLAM testing scenarios under both snowy and sunny conditions.

We used the open-source 4DRT-SLAM algorithm [10] to perform sparse point cloud mapping with the 4D millimeter-wave radar. Notably, no noise points such as snowflakes were observed in the 4D millimeter-wave radar point cloud. However, the sparse nature of the point cloud resulted in poor mapping performance, particularly in terms of height accuracy. While the 4D millimeter-wave radar does provide height information, significant deviations in height were observed during

TABLE VI

DIFFERENT SLAM ALGORITHMS EXHIBIT VARYING ABSOLUTE TRAJECTORY ERRORS (ATE) AND RELATIVE POSE ERRORS (RPE) (UNIT: METERS). WE CONDUCTED ORB-SLAM3 TESTS ON THE SCENES IN THE SECOND AND THIRD ROWS USING BOTH THE LEFT CAMERA AND THE RGB CAMERA. HOWEVER, BUMPS OR LIGHTING CONDITIONS CAUSED TRAJECTORY LOSS (X).

Sequence sensors	Livox-SLAM		4DRT-SLAM		CT-ICP		ORB-SLAM3		R3live		GS-SLAM	
	lidar		4D radar		lidar		rgb		lidar+imu+rgb		rgb+depth	
Metric	ATE	RPE	ATE	RPE	ATE	RPE	ATE	RPE	ATE	RPE	ATE	RPE
L-NB-SU-D	1.20	1.35	11.72	9.38	1.66	0.90	1.81	3.19	3.79	0.81	-	-
L-NB-SU-N	3.13	1.93	12.07	46.73	3.29	2.42	x	x	2.19	1.50	42.23	-
L-B-SU-D	2.14	1.10	6.95	18.87	1.51	0.66	x	x	2.42	0.89	-	-
L-B-SU-N	2.28	1.15	0.47	118.67	2.22	0.82	4.08	4.34	2.31	0.74	-	-
H-BS-SU-D	33.77	16.67	45.84	431.77	126.48	11.31	46.72	12.96	13.95	10.28	249.36	-
H-BS-R-D	24.74	18.67	24.87	334.37	24.94	11.94	34.83	13.46	213.85	10.13	-	-
H-BS-SN-D	44.71	12.68	76.16	241.33	55.85	10.66	39.32	16.45	21.88	7.74	-	-
H-BS-SN-N	39.44	15.01	36.67	295.18	68.02	9.25	287.82	17.97	26.67	9.22	-	-

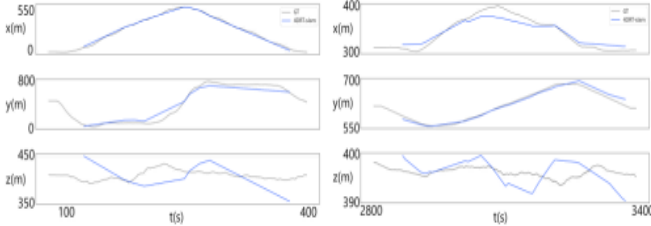


Fig. 9. The figure presents the variation of x, y, and z coordinates over time in two closed-loop scenarios. The blue line represents the 4D millimeter-wave SLAM, while the gray line represents the ground truth (gt). It can be observed that the errors in the x and y coordinates are relatively small, whereas the error in the z-coordinate is significantly larger, and the system is unable to close the loop in closed-loop scenarios.

the mapping process, likely due to the immature transition from 3D to 4D technology. The results of these experiments can be found in Figure 11. Figure 11 highlights the height discrepancies, where we used red circles to mark the starting and ending points, which ideally should be at the same height. Corresponding ground truth data is also provided for reference.

E. Gaussian splatting SLAM

3D Gaussian SLAM is a three-dimensional simultaneous localization and mapping technique based on probabilistic methods. It uses Gaussian distributions to model uncertainty, describing sensor measurement noise and state estimation errors with Gaussian distributions. Through probabilistic theory, the algorithm optimizes the robot's position and the map's accuracy in three-dimensional space. One of its key features is that it can achieve precise localization and mapping using only a camera. However, most existing 3D Gaussian SLAM applications have been focused on indoor environments. While some recent works have explored 3D Gaussian mapping outdoors using a combination of LiDAR and images, we aim to investigate whether a camera alone can accomplish large-scale outdoor mapping tasks.

We tested two outdoor datasets that cover a variety of scenarios, including low-speed and high-speed motion under both daytime and nighttime conditions. Our experiments indicated that using a depth camera, the mapping performance of Gaussian Splatting SLAM in large outdoor scenes is poor. Specifically, in scenarios with low speed and no significant bumps, the Absolute Trajectory Error (ATE) reached 52.594, with a mapping duration of 3 hours. In contrast, in scenarios with high speed and multiple speed bumps, the ATE exceeded 300, with a mapping duration of 2 hours. We believe this is



Fig. 10. On the left is a screenshot of the mapping result provided by monoGS, and on the right is the actual map. The landmark building, the library, has been outlined with a red box, and it can be seen that the mapping effect using depth images for large-scale scenes is poor. Additionally, upon analysis of the pedestrian within the yellow circle, it is observed that the mapping effect for dynamic objects is also poor and there has been no consideration for their removal.

primarily due to the fact that in autonomous driving situations, it is not possible to capture the mapping objects from multiple angles, leading to poorer mapping results. Additionally, due to the larger scale of the scenes, there is more noise in the depth images, which degrades the accuracy of localization. For more details, please refer to Figure 12.

Therefore, optimizing 3D Gaussian SLAM remains a significant challenge so that the system can still perform accurate localization and mapping in outdoor environments using only a camera (including both RGB and depth images), regardless of whether the conditions are low-speed or high-speed. This will be one of the key research directions for enhancing the performance of 3D Gaussian SLAM in future outdoor applications.

F. R3live SLAM

To assess the accuracy of traditional sensor fusion in SLAM under complex and adverse conditions, we conducted experiments using R3LIVE. R3LIVE is a multi-sensor fusion localization and mapping system proposed by the Mars Laboratory at the University of Hong Kong, focusing on real-time performance and robustness. This system tightly couples visual, Inertial Measurement Unit (IMU), and LiDAR data to maintain high-precision pose estimation and map construction capabilities in dynamic environments and complex terrains. R3LIVE comprises two subsystems: the LiDAR-Inertial

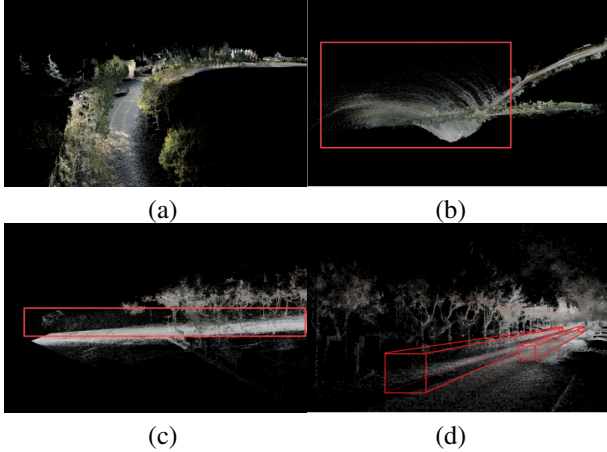


Fig. 11. (a) represents the mapping results of R3LIVE under sunny conditions, which are relatively ideal. (b) illustrates the mapping results of R3LIVE in rainy conditions, where the VIO module's accuracy is compromised due to the camera lens being obscured by rain during the traversal, leading to a decrease in the overall SLAM accuracy. (c) and (d) depict the mapping effects in snowy conditions; (c) contains a significant number of snowflakes within the red frame, while (d)'s red frame highlights erroneous point clouds caused by dynamic vehicles.

Odometry (LIO) and the Visual-Inertial Odometry (VIO). The LIO subsystem (FAST-LIO) utilizes measurements from LiDAR and inertial sensors to construct the geometric structure of the global map, while the VIO subsystem leverages data from visual-inertial sensors to texture the map.

The experimental results indicate that under normal conditions (sunny, daytime), R3LIVE demonstrates high accuracy and superior mapping capabilities. However, during rainy conditions, when the camera lens is obscured by rainwater, R3LIVE does not exhibit superior resistance to such interferences, leading to significant localization errors. In snowy conditions, the presence of a large number of snowflakes and dynamic points such as pedestrians and vehicles integrated into SLAM reduces map construction accuracy. At night, the decrease in precision caused by VIO also interferes with the overall localization accuracy of R3LIVE. Refer to Figure 12 for more details.

V. CONCLUSION

We collected datasets from ground robots and autonomous vehicles under various weather conditions, different road surface conditions, and varying lighting conditions. These datasets combine novel and traditional sensors, contributing to addressing the accuracy challenges of SLAM in extreme conditions. By amassing substantial data and making it publicly available, we aim to provide researchers in the SLAM field with more options for their studies.

We evaluated mature and excellent SLAM algorithms based on various sensor types using the collected datasets. Experiments show that the positioning accuracy of these algorithms still requires improvement under certain extreme conditions. In the future, we plan to enhance SLAM's adaptability to various extreme environments by leveraging multi-sensor fusion methods.

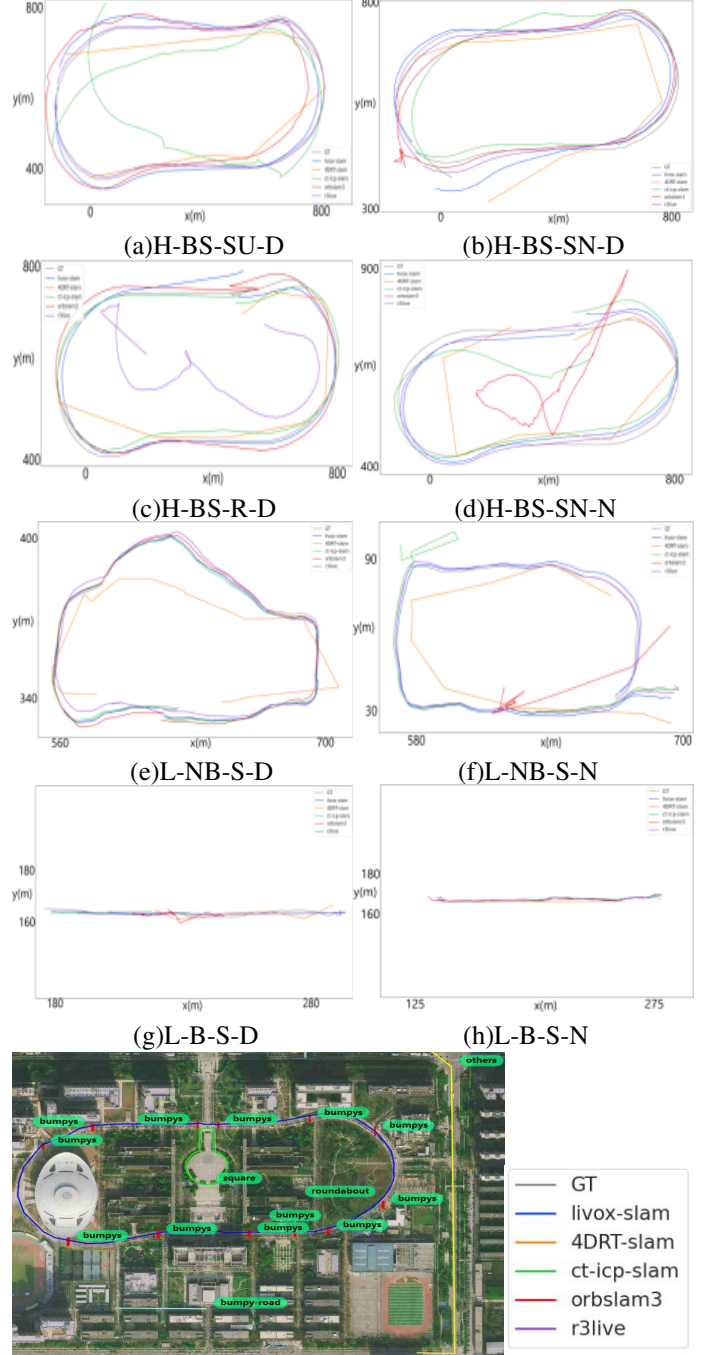


Fig. 12. We conducted tests on data collected under eight different weather, lighting, and road surface conditions, comparing the trajectories generated by two LiDAR SLAM algorithms, one visual SLAM algorithm, one 4D millimeter-wave radar SLAM algorithm, and one tightly-coupled laser, camera, IMU algorithm. In various scenarios, the SLAM positioning trajectories of individual sensors were poor. We have also included the actual terrain along with the trajectory maps, annotations, and legends below, with the trajectories including the locations of speed bumps.

LICENSE

This dataset is licensed under CC BY-NC-ND 4.0. For commercial use, please contact us for permission.

REFERENCES

- [1] Pritsker, A. Alan B. (1984) Introduction to Simulation and SLAM II. Halsted Press.

- [2] Singandhupe, A., La, H. M. (2019) A review of SLAM techniques and security in autonomous driving. In 2019 third IEEE international conference on robotic computing (IRC) (pp. 1-6). IEEE.
- [3] Cadena, C., Carlone, L., Carrillo, H., Latif, Y., Scaramuzza, D., Neira, J., ... Leonard, J. J. (2016) Past, present, and future of simultaneous localization and mapping: Toward the robust-perception age. *IEEE Transactions on Robotics*, 32(6), 1309-1332.
- [4] Xu, X., Zhang, Y., Liu, Z., Lin, Y., Zhang, J., Tang, Y. (2022) A review of multi-sensor fusion SLAM systems based on 3D LIDAR. *Remote Sensing*, 14(12), 2835.
- [5] Wang, B., Zhuang, Y., El-Bendary, N. (2023) 4D RADAR/IMU/GNSS integrated positioning and mapping for large-scale environments. *The International Archives of the Photogrammetry, Remote Sensing and Spatial Information Sciences*, 48, 1223-1228.
- [6] Handa, A., Whelan, T., McDonald, J., Davison, A. J. (2014, May) A benchmark for RGB-D visual odometry, 3D reconstruction and SLAM. In 2014 IEEE international conference on robotics and automation (ICRA) (pp. 1524-1531). IEEE.
- [7] Wen, W., Zhou, Y., Zhang, G., Fahandez-Saadi, S., Bai, X., Zhan, W., ... Hsu, L. T. (2020, May) UrbanLoco: A full sensor suite dataset for mapping and localization in urban scenes. In 2020 IEEE international conference on robotics and automation (ICRA) (pp. 2310-2316). IEEE.
- [8] Wenzel, P., Wang, R., Yang, N., Cheng, Q., Khan, Q., von Stumberg, L., ... Cremers, D. (2021) 4Seasons: A cross-season dataset for multi-weather SLAM in autonomous driving. In *Pattern Recognition: 42nd DAGM German Conference, DAGM GCPR 2020, Tübingen, Germany, September 28–October 1, 2020, Proceedings* 42 (pp. 404-417). Springer International Publishing.
- [9] Ligocki, A., Jelinek, A., Zalud, L. (2020, May) Brno urban dataset—the new data for self-driving agents and mapping tasks. In 2020 IEEE International Conference on Robotics and Automation (ICRA) (pp. 3284-3290). IEEE.
- [10] Zhang, J., Zhuge, H., Liu, Y., Peng, G., Wu, Z., Zhang, H., ... Wang, D. (2023, September) Ntu4dradlm: 4d radar-centric multi-modal dataset for localization and mapping. In 2023 IEEE 26th International Conference on Intelligent Transportation Systems (ITSC) (pp. 4291-4296). IEEE.
- [11] Schramm, S., Rangel, J., Kroll, A. (2018) Data fusion for 3D thermal imaging using depth and stereo camera for robust self-localization. In 2018 IEEE Sensors Applications Symposium (SAS) (pp. 1-6). IEEE.
- [12] Zhao, T., Xie, Y., Ding, M. et al. (2024) A road surface reconstruction dataset for autonomous driving. *Sci Data*, 11, 459.
- [13] Zheng, C., Ding, M., He, H., Chen, X., Zhao, T. (2022) Fast-livo: Fast and tightly-coupled sparse-direct lidar-inertial-visual odometry. In 2022 IEEE/RSJ International Conference on Intelligent Robots and Systems (IROS) (pp. 1-6). IEEE.
- [14] Lin, J., Zhang, F. (2022) R 3 LIVE: A Robust, Real-time, RGB-colored, LiDAR-Inertial-Visual tightly-coupled state Estimation and mapping package. In 2022 International Conference on Robotics and Automation (ICRA) (pp. 1-6). IEEE.
- [15] Campos, C., Elvira, R., Rodríguez, J. J. G., Montiel, J. M. M., Tardós, J. D. (2021) Orb-slam3: An accurate open-source library for visual, visual-inertial, and multimap SLAM. *IEEE Transactions on Robotics*, 37(6), 1874-1890.
- [16] Endres, F., Hess, J., Engelhard, N., Stuckler, J., Sturm, J., Burgard, W. (2013) 3-D mapping with an RGB-D camera. *IEEE Transactions on Robotics*, 30(1), 177-187.
- [17] Cheng, J., Zhou, J., Liu, W., Han, X., Xie, Q., Zhou, C. (2020) DM-SLAM: A feature-based SLAM system for rigid dynamic scenes. *ISPRS International Journal of Geo-Information*, 9(4), 202.
- [18] Shan, T., Englot, B., Meyers, D., Wang, W., Ratti, C., Rus, D. (2020) Lio-sam: Tightly-coupled lidar inertial odometry via smoothing and mapping. In 2020 IEEE/RSJ international conference on intelligent robots and systems (IROS) (pp. 1-6). IEEE.
- [19] Zhao, T., Lu, X., Ye, T. (2023) A comprehensive implementation of road surface classification for vehicle driving assistance: Dataset, models, and deployment. *IEEE Transactions on Intelligent Transportation Systems*, 24(8), 8361-8370.
- [20] Geiger, A., Lenz, P., Urtasun, R. (2012) Are we ready for autonomous driving? the kitti vision benchmark suite. In 2012 IEEE conference on computer vision and pattern recognition (pp. 1-8). IEEE.
- [21] Burri, M., Nikolic, J., Gohl, P., Schneider, T., Rehder, J., Omari, S., ... Scaramuzza, D. (2016) The EuRoC micro aerial vehicle datasets. *The International Journal of Robotics Research*, 35(10), 1157-1163.
- [22] Schubert, D., Goll, T., Demmel, N., Usenko, V., Stücker, J., Cremers, D. (2018) The TUM VI benchmark for evaluating visual-inertial odometry. In 2018 IEEE/RSJ International Conference on Intelligent Robots and Systems (IROS) (pp. 1-6). IEEE.
- [23] Wenzel, P., Whelan, T., Khan, Q., von Stumberg, L., Cremers, D. (2021) 4Seasons: A cross-season dataset for multi-weather SLAM in autonomous driving. *Pattern Recognition: 42nd DAGM German Conference, DAGM GCPR 2020, Tübingen, Germany, September 28–October 1, 2020, Proceedings* 42. Springer International Publishing.
- [24] Yin, J., Xie, Q., Wu, Z., Wu, Y., Xie, Q., Huang, G., ... Gao, F. (2021) M2DGR: A multi-sensor and multi-scenario SLAM dataset for ground robots. *IEEE Robotics and Automation Letters*, 7(2), 2266-2273.
- [25] Sattler, T., Maddern, W., Toft, C., Torii, A., Hammarstrand, L., Stenborg, E., ... Pollefeys, M. (2018) Benchmarking 6DoF outdoor visual localization in changing conditions. In *Proceedings of the IEEE conference on computer vision and pattern recognition* (pp. 1-8). IEEE.
- [26] Zhang, X., Li, F., Shen, Y., Zhao, T., Chen, L., Chen, X. (2023) Dual radar: A multi-modal dataset with dual 4D radar for autonomous driving. *arXiv preprint arXiv:2310.07602*.
- [27] Lin, J., Zhang, F. (2020) LOAM Livox: A fast, robust, high-precision LiDAR odometry and mapping package for LiDARs of small FoV. In 2020 IEEE International Conference on Robotics and Automation (ICRA) (pp. 1-6). IEEE.
- [28] Zhang, J., Keramat, F., Yu, X., Hernández, D. M., Queralta, J. P., Westerlund, T. (2022) Distributed robotic systems in the edge-cloud continuum with ROS 2: A review on novel architectures and technology readiness. In *Proceedings of the 2022 Seventh International Conference on Fog and Mobile Edge Computing (FMEC)*, Paris, France, 12–15 December 2022.
- [29] Liu, T., Kang, H., Chen, C. (2023) ORB-Livox: A real-time dynamic system for fruit detection and localization. *Computers and Electronics in Agriculture*, 209, 107834.
- [30] Shin, U., Kim, J., Oh, J., Kim, T., Lee, H., Choi, J. (2021) Self-supervised depth and ego-motion estimation for monocular thermal video using multi-spectral consistency loss. *IEEE Robotics and Automation Letters*, 7(2), 1103-1110.
- [31] Paris, A., Lopez, B. T., How, J. P. (2020) Dynamic landing of an autonomous quadrotor on a moving platform in turbulent wind conditions. In 2020 IEEE International Conference on Robotics and Automation (ICRA) (pp. 1-8). IEEE.
- [32] Rehder, J., Nikolic, J., Schneider, T., Hinzmann, T., Scaramuzza, D. (2016) Extending Kalibr: Calibrating the extrinsics of multiple IMUs and of individual axes. In 2016 IEEE International Conference on Robotics and Automation (ICRA) (pp. 1-8). IEEE.
- [33] Prokhorov, D., Blumenstein, M., Ye, X., Morison, D., Paul, G. (2019) Measuring robustness of visual SLAM. In 2019 16th International conference on machine vision applications (MVA) (pp. 1-6). IEEE.
- [34] Dellenbach, P., Stoll, M., Cadena, C., Siegwart, R. (2022) CT-ICP: Real-time elastic LiDAR odometry with loop closure. In 2022 International Conference on Robotics and Automation (ICRA) (pp. 1-8). IEEE.
- [35] Lin, J., Zhang, F., Zou, D., Pei, L. (2021) R²LIVE: A robust, real-time, LiDAR-inertial-visual tightly-coupled state estimator and mapping. *IEEE Robotics and Automation Letters*, 6(4), 7469-7476.
- [36] Tu, Z., Ye, Q., Gao, L., Xiao, Z., Cheng, X. (2022) RGBT salient object detection: A large-scale dataset and benchmark. *IEEE Transactions on Multimedia*, 1-12.
- [37] Zhao, Y., Lu, X., Ye, T. (2023) One robust loosely coupled 4D millimeter-wave image radar SLAM method. No. 2023-01-7051. SAE Technical Paper.
- [38] W. Maddern, G. Pascoe, C. Linegar and P. Newman, "1 Year, 1000km: The Oxford RobotCar Dataset", *The International Journal of Robotics Research (IJRR)*, 2016.